SUPPLEMENTARY FIGURE LEGENDS

Supplementary Figure S1: MALDI-TOF MS profiles of the permethylated *O*-linked glycans derived from SRECs. For complete annotation of the spectrum, see Table S2. Data were obtained from the 35% acetonitrile fraction and all molecular ions are present in sodiated form ([M+Na]+).

Supplementary Figure S2: MALDI-TOF/TOF MS/MS spectrum of the permethylated *N*-glycan at *m/z* 3054.8, derived from SRECs. Assignments of the key fragment ions generated and alternative antennal arrangements are shown.

Supplementary Figure S3: MALDI-TOF MS profiles of the permethylated *N*-linked glycans derived from SRECs after digestion with *endo-β*-galactosidase. Data were obtained from the 50% acetonitrile fraction and all molecular ions are present in sodiated form ($[M+Na]^+$). Insert represents low molecular weight region from the 35% acetonitrile fraction and all molecular ions are present in sodiated form ($[M+Na]^+$).

Supplementary Figure S4: MALDI-TOF MS profiles of the permethylated *N*-glycans (A-C) and *O*-glycans (D-F) from untreated SRECs (A and D), from SRECs grown in the presence of 0.1mM ManNGc for 2 days prior to analysis (B and E) and from SRECs grown in the presence of 0.1mM ManNGc and 5mM ManNAc for 2 days prior to analysis (C and F). *N*-glycan data were obtained from the 50% acetonitrile fraction and *O*-glycan data were obtained from the 35% acetonitrile. All molecular ions are present in sodiated form ([M+Na]+). Sialylated species are annotated in red. A 30 Da increment satellite signals was observed for all the *N*-glycans, not just those containing Sia (Fig. S4 B, C). Similar satellite signals were observed in ManNGc alone and both ManNAc and ManNGc-treated *O*-glycans (Fig. S4 E, F).

Supplementary Figure S5: MALDI-TOF/TOF MS/MS spectrum of the permethylated *O*-glycan at *m/z* 925, derived from control SRECs (A), from SRECs grown in the presence of 0.1mM ManNGc for 2 days prior to analysis (B), and from SRECs grown in the presence of 0.1mM ManNGc and 5mM ManNAc for 2 days prior to analysis (C). Assignments of the fragment ions generated are shown. The data shows the MS/MS spectra of the mono-sialyated core 1 *O*-glycan (NeuGcHexHexNAc) from untreated SRECs, cells treated with ManNGc alone, or cells treated with both precursors. The presence of the Z ion at *m/z* 298 and the C ion at *m/z* 650 plus the ZY ion at *m/z* 284 and the Z ion at *m/z* 689 are consistent with a mono-NeuGc core 1 *O*-glycan in which the NeuGc can be on either the Gal or GalNAc (A). The MS/MS analysis of the same molecular ion peak at *m/z* 925 from SREC cells treated with ManNGc alone or with both ManNGc and ManNAc precursors produced complex spectra and indicated the presence of an additional species with composition NeuAcHexHexNAc+30, as indicated by the additional B ion at *m/z* 398 and C ion at *m/z* 620. The presence of an additional Y ion at *m/z* 550, plus the lack of +30 satellite peaks associated with the C ion at *m/z* 650, indicates that the +30 addition is associated with the reducing end HexNAc residue. By comparison of the ratio of the Y ions at *m/z* 520 and 550 it can be seen that the NeuGcHexHexNAc structure increases in abundance in the SREC cells treated with ManNGc alone compared to cells treated with both precursors (B,C). Similar data were obtained from MS/MS analysis of SREC *N*-glycans treated with ManNGc alone or with both ManNGc and ManNAc precursors. Taken together, these data indicate that for non-sialylated glycans the +30 addition was associated with HexNAc residues and for sialylated glycans the +30 addition was associated with both a switch from NeuAc to NeuGc and modification of HexNAc residues.

Unexpectedly, in addition to modulating sialic acids, mannosamine precursors also altered GlcNAc and GalNAc moieties on SREC *N*- and *O*-glycans, respectively. Other studies have examined the effects of precursors (1-5), but have analyzed only the effect on sialylated structures (not on the pool of *N*- and

O-glycans), and as such have not observed the unique changes in GlcNAc and GalNAc (6). Luchansky *et al*. showed that expression of GlcNAc 2-epimerase in Jurkat cells suppresses sialic acid production in response to exogenous addition of ManNAc and analogs of ManNAc (7). The interpretation of our results is that GlcNAc 2-epimerase converts ManNGc into GlcNGc, which is then incorporated into *N*-glycans. GlcNGc is also converted to UDP-GalNGc in several steps, which is incorporated into *O*-glycans. Another possible explanation for the observed difference between our results and those of others could be that GlcNAc 2-epimerase is permissive for ManNGc, but not for more distant structural analogs of ManNAc, such as *N*-levulinoylmannosamine or 3-azido-3-deoxymannosamine. The decrease in virus infectivity after ManNGc treatment of SRECs could be due to conversion of NeuAc to NeuGc, from GlcNAc/GalNAc to GlcNGc/GalNGc (for *N*- and *O*-linked glycans, respectively), or both. However, we believe the most likely explanation is a conversion from NeuAc to NeuGc. First, GlcNAc/GalNAc remained the majority species throughout our studies (Fig. S4). Second, when SRECs are treated with both precursors simultaneously, the 30 Da increment satellite signals are present, indicating the presence of GlcNGc/GalNGc (Fig. S4). However, in these cells the virus infectivity levels are similar to levels in untreated cells (Fig. 4), demonstrating that the amount of GlcNGc/GalNGc in cells treated with both precursors does not affect infectivity. Third, structures of virus HA complexed with sialylated glycans indicate that the GlcNAc moiety either does not make substantial interactions with HA (8-11) or the GlcNAc makes only one interaction, with HA residue 190 contacting the acetamido nitrogen of GlcNAc (12, 13). This interaction is maintained in both GlcNAc/GalNAc and GlcNGc/GalNGc, so conversion to GlcNGc/GalNGc would not be expected to have a substantial impact. Thus, the *N*-acyl group of NeuAc appears to play a larger role in HA-Sia binding than the *N*-acyl group of GlcNAc/GlcNGc, indicating that the infectivity changes we observe are likely due to the conversion of NeuAc to NeuGc.

REFERENCES

1. Collins, B. E., Fralich, T. J., Itonori, S., Ichikawa, Y., and Schnaar, R. L. (2000) *Glycobiology* **10**, 11-20
2. Bardor, M., Nguyen, D. H., Diaz, S., and Varki, A. (2005) *J. Biol. Chem.* **280**, 4228-4237
3. Keppler, O. T., Herrmann, M., von der Lieth, C. W., Stehling, P., Reutter, W., and Pawlita, M. (1998)
4. Keppler, O. T., Stehling, P., Herrmann, M., Kayser, H., Grunow, D., Reutter, W., and Pawlita, M. (1995) *J. Biol. Chem.* **270**, 1308-1314
5. Oetke, C., Brossmer, R., Mantey, L. R., Hinderlich, S., Isecke, R., Reutter, W., Keppler, O. T., and Pawlita, M. (2002) *J. Biol. Chem.* **277**, 6688-6695
6. Jacobs, C. L., Goon, S., Yarema, K. J., Hinderlich, S., Hang, H. C., Chai, D. H., and Bertozzi, C. R. (2001) *Biochemistry* **40**, 12864-12874
7. Luchansky, S. J., Yarema, K. J., Takahashi, S., and Bertozzi, C. R. (2003) *J. Biol. Chem.* **278**, 8035-8042
8. Liu, J., Stevens, D. J., Haire, L. F., Walker, P. A., Coombs, P. J., Russell, R. J., Gamblin, S. J., and Skehel, J. J. (2009) *Proc. Natl. Acad. Sci. U. S. A.* **106**, 17175-17180
9. Ha, Y., Stevens, D. J., Skehel, J. J., and Wiley, D. C. (2003) *Virology* **309**, 209-218
10. Eisen, M. B., Sabesan, S., Skehel, J. J., and Wiley, D. C. (1997) *Virology* **232**, 19-31
11. Ha, Y., Stevens, D. J., Skehel, J. J., and Wiley, D. C. (2001) *Proc. Natl. Acad. Sci. U. S. A.* **98**, 11181-11186
12. Gamblin, S. J., Haire, L. F., Russell, R. J. *et al.* (2004) *Science* **303**, 1838-1842
13. Russell, R. J., Stevens, D. J., Haire, L. F., Gamblin, S. J., and Skehel, J. J. (2006) *Glycoconj. J.* **23**, 85-92

SUPPLEMENTARY TABLE LEGENDS

Supplementary Table S1: Compositional assignments and masses of singly charged sodiated molecular ions, $[M+Na]^+$, observed in MALDI-MS spectra of permethylated *N*-glycans derived from the SRECs analyzed within this paper.

Supplementary Table S2: Compositional assignments and masses of singly charged sodiated molecular ions, $[M+Na]^+$, observed in MALDI-MS spectra of permethylated *O*-glycans derived from the SRECs analyzed within this paper.

Supplementary Table S3: GC-MS analyses of partially methylated alditol acetates obtained from the 50% acetonitrile fraction of PNGase F released *N*-glycans of SRECs.

Supplementary Table S4: Structure and relative fluorescent units of Sw/MN and Sw/ONT binding to all 465 glycans on the glycan microarray.

Figure S1

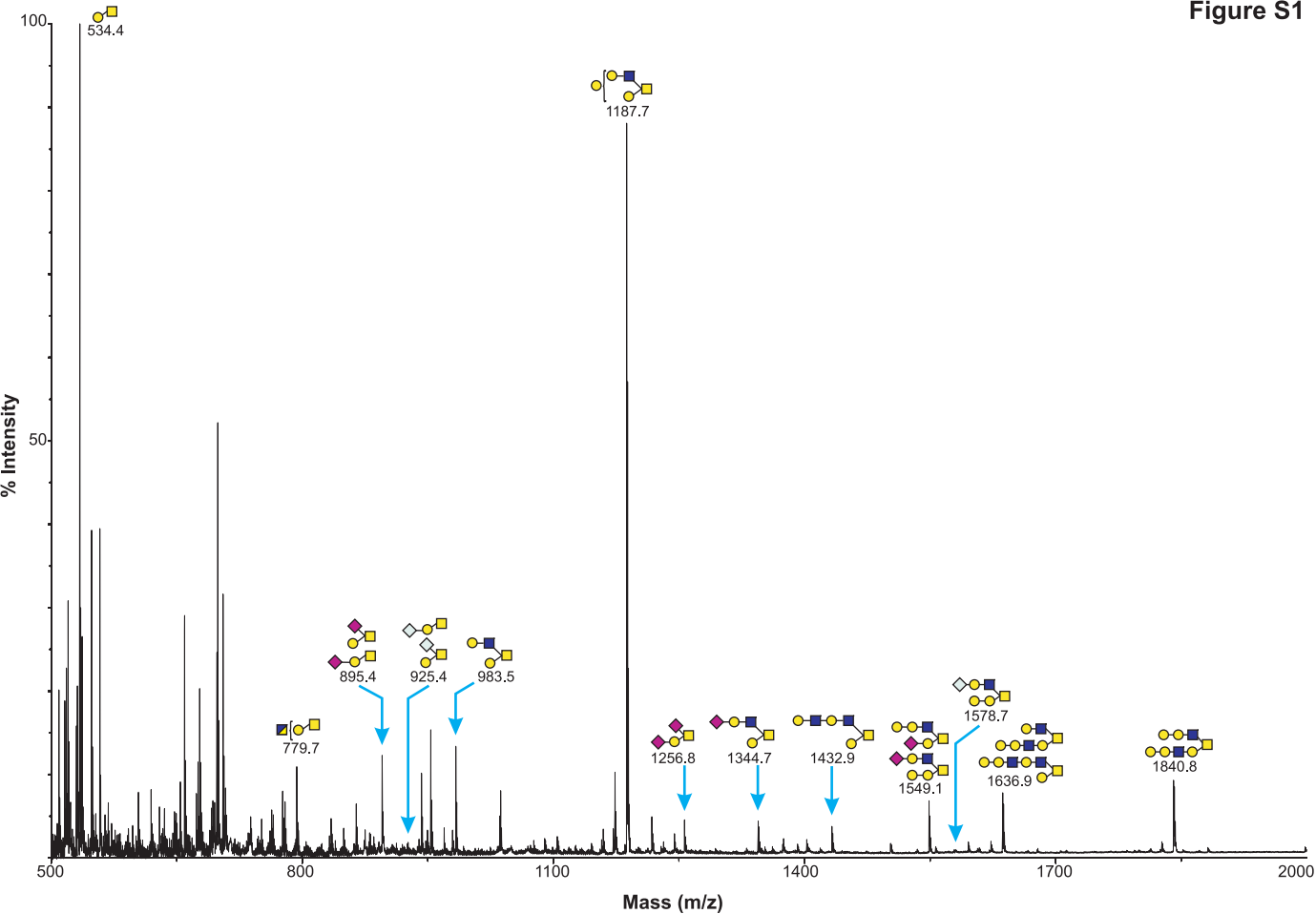
100
50
% Intensity
500
800
1100
1400
1700
2000
Mass (m/z)
534.4
1187.7
779.7
895.4
925.4
983.5
1256.8
1344.7
1432.9
1549.1
1578.7
1636.9
1840.8

Figure S2

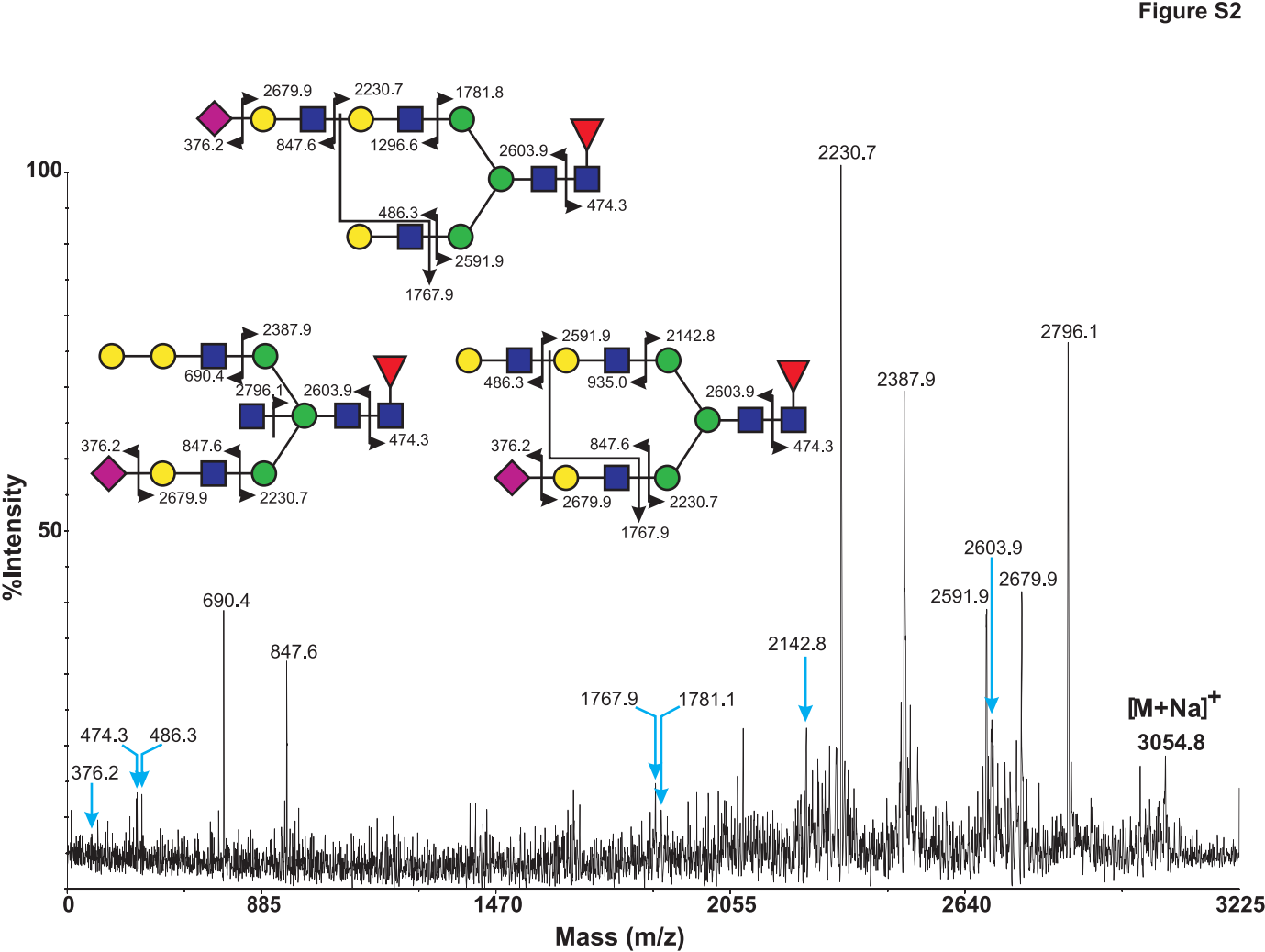
2679.9
2230.7
1781.8
376.2
847.6
1296.6
2603.9
474.3
486.3
2591.9
1767.9
2387.9
690.4
2796.1
2603.9
474.3
376.2
847.6
2679.9
2230.7
2591.9
2142.8
486.3
935.0
2603.9
474.3
376.2
847.6
2679.9
2230.7
1767.9
100
50
%Intensity
2230.7
2796.1
2387.9
2603.9
2679.9
2591.9
690.4
847.6
2142.8
1767.9
1781.1
474.3
486.3
376.2
[M+Na]+
3054.8
0
885
1470
2055
2640
3225
Mass (m/z)

Figure S3

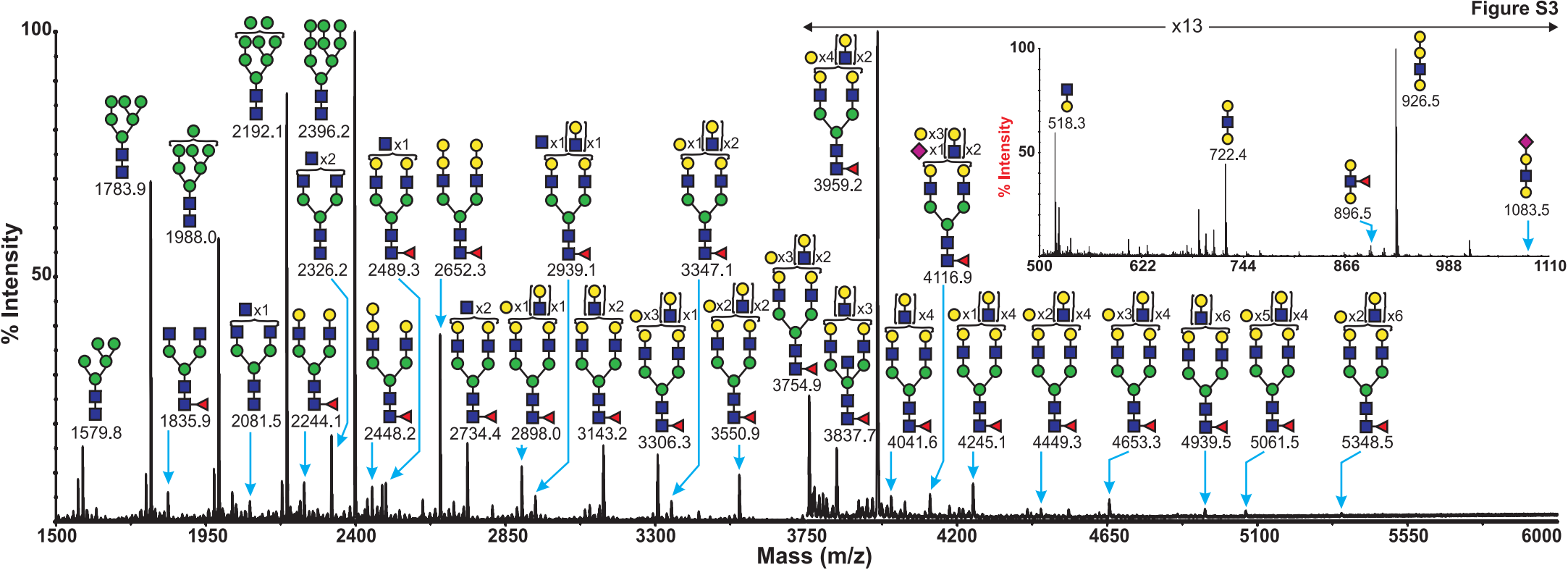
% Intensity
Mass (m/z)
100
50
1500
1950
2400
2850
3300
3750
4200
4650
5100
5550
6000
1579.8
1783.9
1835.9
1988.0
2081.5
2192.1
2244.1
2326.2
2396.2
2448.2
2489.3
2652.3
2734.4
2898.0
2939.1
3143.2
3306.3
3347.1
3550.9
3754.9
3837.7
3959.2
4041.6
4116.9
4245.1
4449.3
4653.3
4939.5
5061.5
5348.5
x13
518.3
722.4
896.5
926.5
1083.5
500
622
744
866
988
1110

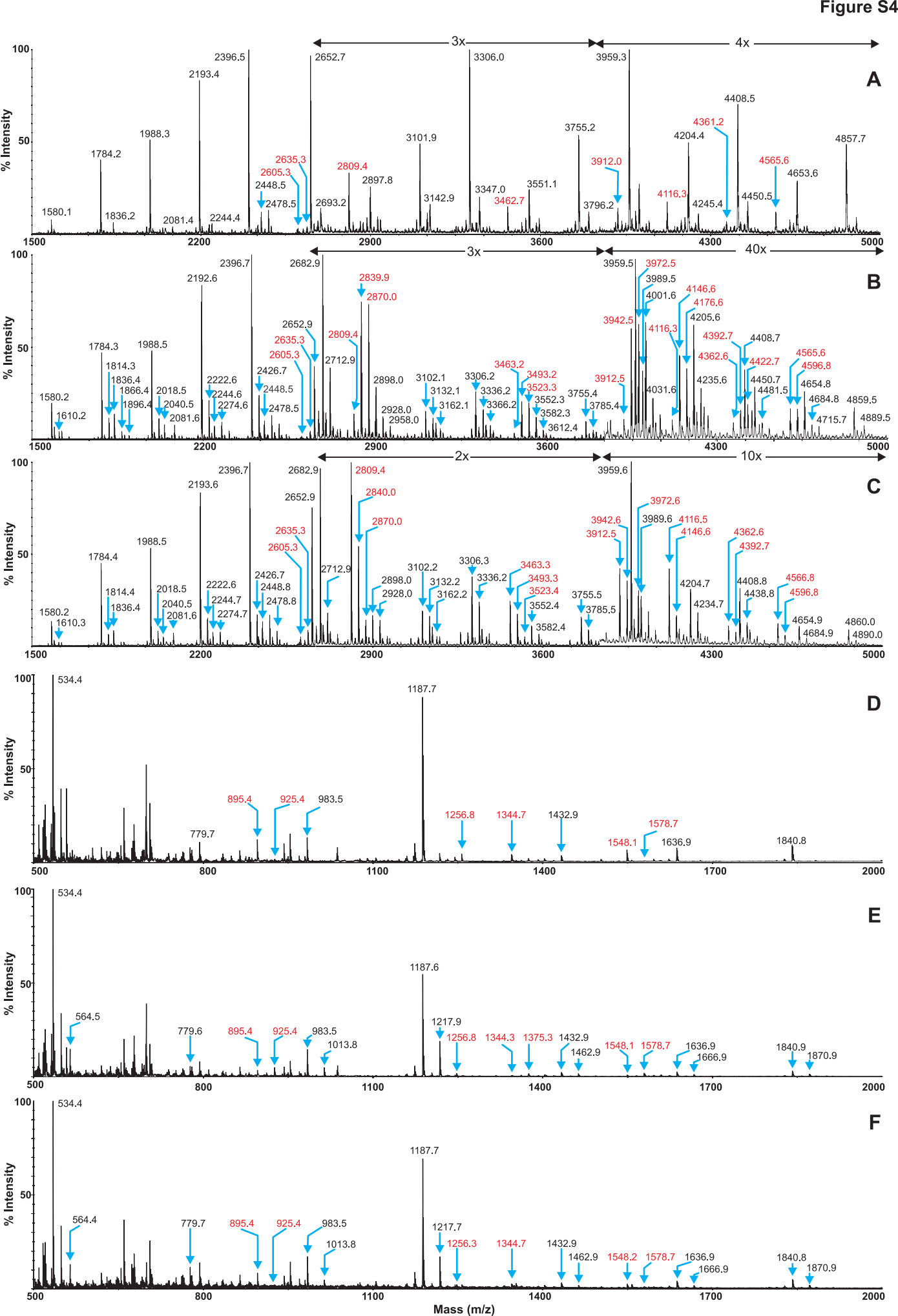
A
3x
4x
B
3x
40x
C
2x
10x
D
E
F
% Intensity
Mass (m/z)

Figure S5

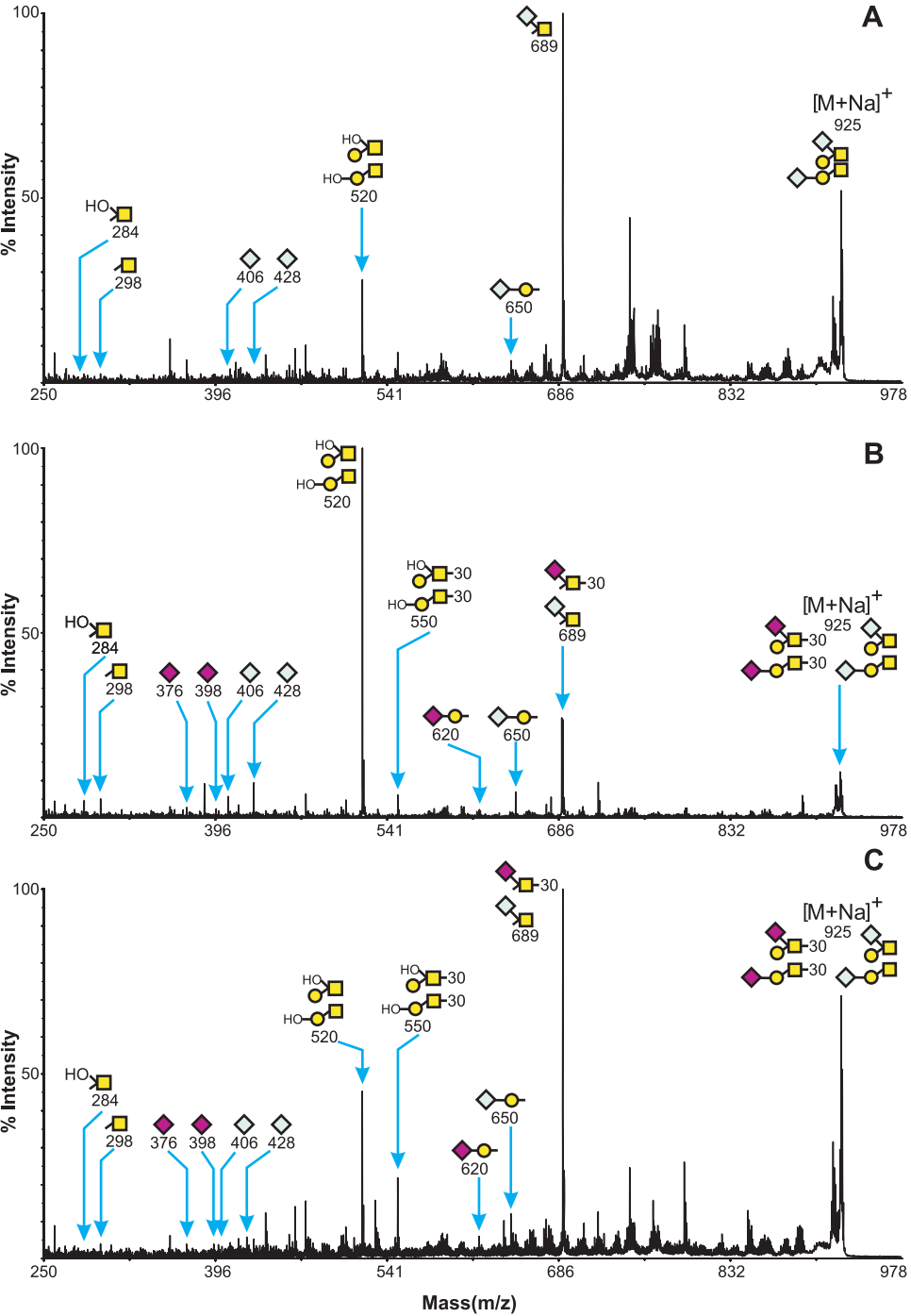
A
B
C
% Intensity
100
50
250
396
541
686
832
978
Mass(m/z)
[M+Na]+
925
689
520
284
298
406
428
650
376
398
620
550
30